INT. J. NUM. METH. HEAT FLUID FLOW, VOL. 5, 813–827 (1995)

FAST FOURIER TRANSFORM OF SPECTRAL BOUNDARY ELEMENTS FOR TRANSIENT HEAT CONDUCTION

L. R. HILL and T. N. FARRIS

School of Aeronautics and Astronautics Purdue University, 1282 Grissom Hall, West Lafayette, IN 47907-1282, USA

ABSTRACT

The spectral boundary element method for solving two-dimensional transient heat conduction problems is developed. This method is combined with the fast Fourier transform (FFT) to convert the solution between the time and frequency domains. The fundamental solutions in the frequency domain, required for the present method, are discussed. The resulting line integrations in the frequency domain are discretized using constant boundary elements and used in a Fortran boundary element program. Three examples are used to illustrate the accuracy and effectiveness of the method in both the frequency and time domains. First, the frequency domain solution procedure is verified using the steady-state example of a semi-infinite half space with a heat flux applied to a patch of the surface. This spectral boundary element method is then applied to the problem of a circular hole in an infinite solid subjected to a time-varying heat flux, and solutions in both the frequency and time domains are presented. Finally, the method is used to solve the circular hole problem with a convection boundary condition. The accurary of these results leads to the conclusion that the spectral boundary element method in conjunction with the FFT is a viable option for transient problems. In addition, this spectral approach naturally produces frequence domain information which is itself of interest.

KEY WORDS Fast Fourier transform Spectral boundary elements

INTRODUCTION

The boundary element method (BEM) is a numerical procedure used to solve partial differential equations. For boundary initial-value problems, the BEM requires knowledge of the boundary conditions and initial conditions of the domain of interest. This method requires only that the boundary be partitioned into elements in order to determine the solution, whereas the finite element method requires that the domain itself be discretized. As a result, two-dimensional problems require a numerical solution for only a one-dimensional integral equation. The BEM is particularly useful when the region of interest is much smaller than the entire domain, or when the results are desired only on the surface. However, conditions interior to the boundary can be determined as a sum once the boundary values have been calculated. Heat conduction problems involving sliding contact, layered materials, or near surface defects lend themselves to efficient solution by the BEM.

The boundary element method utilizes the weighted residual technique to minimize the error in the solution of a partial differential equation. The weighting functions can be selected arbitrarily, but careful selection of the function will produce better results in the minimization[1,2,3]. The boundary element method described herein forms the basis for the development of a Fortran DYNamic Boundary Element Method Program (DYNBEMP). In order to perform the analysis for transient problems, a choice was made as to the treatment of time in the governing equation.

0961–5539/95/090813–16$2.00

Received January 1994
Revised June 1994

Three procedures have been utilized by others for BEM programs: the time-marching method, the Laplace transform method, and the Fourier transform method. A summary of these three methods follows, and Manolis[4] and Beskos[5] discuss further the differences in these procedures.

The time-marching approach solves the problem in the time domain directly, utilizing such methods as finite difference or time-dependent fundamental solutions[6]. The main advantage of this procedure is that it is simple and straightforward. Disadvantages involve possible numerical instability for small time steps and possible lengthy time to solution. Solutions found using this procedure are in general more accurate early in the time period of interest than later, since errors in the solution accumulate as time progresses.

Many authors have used the Laplace transform to remove time dependency in diffusion equations with applications other than heat conduction, such as unsteady flow in aquifers[7,8] and soil consolidation[9], but Rizzo and Shippy[10] were the first to use a boundary element formulation for transient heat conduction problems. They used the Laplace transform and the inverse transform to obtain time history solutions. Since that time much research has been conducted in this area[11,12]. The main advantage of the Laplace transform method is that a reduction in dimensionality is effectively achieved provided that the initial conditions satisfy Laplace's equation. In addition, the solutions for steady state problems are easily determined since they require no inversion to recover the time domain results. Its main drawback is that good knowledge of the expected solution behaviour is needed to select the transform parameter s. This approach is not efficient for problems of complex time history since the process is basically a curve-fit and can be unstable if too many values of s are chosen or inaccurate if too few are used[13].

The method of solution using the Fourier transform is similar to that using the Laplace transform and has also been applied to a variety of problems, including heat conduction, thermoelasticity, and fluid flow[14]. The Laplace transform parameter s corresponds to the complex frequency $i\omega$ in the Fourier transform, where $i=\sqrt{-1}$, indicating that the Fourier transform requires solutions be found in the complex domain. The main difference in the two methods is the manner in which the transforms are inverted. Specifically, here the fast Fourier transform (FFT) is available for efficient inversion from the frequency domain to the time domain[15]. The advantages of this Fourier method are the same as for Laplace method mentioned above, and only one major disadvantage of the procedure exists. For problems where the time window of interest is long and the time history more complex, a small time step and a large number of transform points are needed to recover accurate solutions, requiring large amounts of CPU time. However, this problem has been overcome using a frequency selection procedure discussed later in this paper. In addition, the present technique is ideally suited to massively parallel computation.

DYNBEMP uses this Fourier transform method, in conjunction with the FFT, to convert from the time domain to the frequency domain and back. This type of derivation and implementation follows the static solution procedure, since the transient problem is redefined as a series of pseudo-static ones. In addition, the frequency domain development naturally provides information on the dynamic properties of the system, which are often themselves of interest[16]. The purpose of this paper is to assess the effectiveness of the FFT as a tool appropriate for combination with the spectral boundary element method, specifically as applied to transient heat conduction problems.

SPECTRAL BEM DEVELOPMENT

Governing integral equation

The governing equation for heat conduction problems can be expressed, in either one, two, or three dimensions[17], as,

$$\nabla^2 T=\frac{1}{\kappa}\frac{\partial T}{\partial t} \quad \text{in } \Omega \tag{1}$$

where T is temperature, Ω represents the domain of interest, $\kappa = k/\rho c$ is thermal diffusivity, k is thermal conductivity, ρ is density, c is specific heat, ∇^2 is the Laplacian operator, and t is time.

Equation (1), which is transient, is transformed into the frequency domain using the FFT. For two-dimensional problems, the temperature is written in spectral form as,

$$T(x, y, t) = \sum^{n} \hat{T}_n(x, y, \omega_n)\, e^{i\omega_n t} \tag{2}$$

where $i = \sqrt{-1}$ and ω_n are discrete frequencies of an FFT spectrum. Substitution of (2) into (1) yields,

$$\nabla^2 \hat{T}_n - \frac{i\omega_n}{\kappa} \hat{T}_n = 0 \tag{3}$$

Equation (3), also known as the Helmholz equation, becomes the basis for the BEM formulation for the heat conduction problem in the frequency domain. It is noted that $\hat{T}$ is a complex-valued temperature in the frequency domain. From this point forward, the carat and the subscript on the discrete frequency terms will be dropped for neatness. Clarification will be made, if necessary, to distinguish the time and frequency domains.

The three types of boundary conditions for the Helmholz problem can now be considered. The first type, referred to as essential, is $T = \bar{T}$ on Γ_1. The second, called the natural condition, is $q = \bar{q}$ on Γ_2, where $q = k(dT/dn)$ is the component of the heat flux in the direction of the outward normal to Γ_2, the boundary of Ω. The barred terms in these conditions represent known quantities on their respective boundaries. The third type is a combination of T and q which occurs in convective boundary conditions. For the results contained herein, the convective relation used is $q = -h_f(T - T_f)$ where h_f is the coefficient of heat transfer across the interface, Γ_3, between Ω and the ambient domain and T_f is the ambient temperature. The known boundary value in this case is T_f and the unknown variable used is the temperature, T on Γ_3. The flux is determined after the solution of the BEM using the convective relation. For a well-posed boundary value problem, Γ_1, Γ_2, Γ_3 must cover all of Γ without any overlap, as in *Figure 1*.

The weighted residual method is used on the governing equation of heat conduction to produce the boundary integral equation. This procedure and resulting Fortran code rely on the work of Hucker and Farris[18]. The weighted residual method is accomplished by multiplying (2) by an arbitrary function T^* and integrating across the domain to obtain,

$$\int_{\Omega} T^* \left(\nabla^2 T - \frac{i\omega}{\kappa} T \right) d\Omega = 0 \tag{4}$$

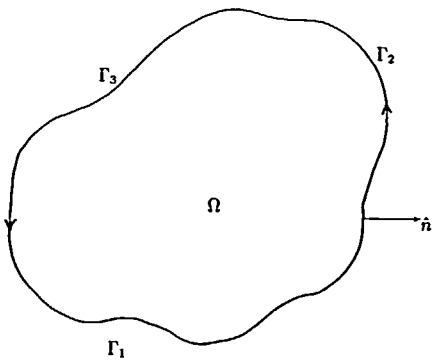

Figure 1 Typical boundary element problem geometry, with Ω indicating the domain of interest, Γ_1 the boundary on which temperatures are known, Γ_2 the boundary on which fluxes are known, Γ_3 where convection occurs, and $\hat{n}$ representing the outward unit normal

Application of Green's first and second theorems to (4) and rearranging yields,

$$\int_\Omega T\left(\nabla^2 T^* - \frac{i\omega}{\kappa} T^*\right) d\Omega + \int_\Gamma \frac{dT}{dn} T^* \, d\Gamma - \int_\Gamma \frac{dT^*}{dn} T \, d\Gamma = 0 \tag{5}$$

The weighting function T^* must satisfy the Helmholz equation (3) and the smoothness requirements have placed on it by the use of Green's theorems. Green's theorems require that T^* have continuous derivatives of at least the second order, interpreted in the sense of generalized functions. The fundamental equation for the two-dimensional Helmholz problem is expressed as,

$$\nabla^2 T^*(x, y, \xi, \eta, \omega) - \frac{i\omega}{\kappa} T^* + \Delta = 0 \tag{6}$$

where Δ is the Dirac delta function with a source point at (ξ, η). This represents a point source of heat at (ξ, η) oscillating with the frequency ω. The fundamental solution to (6) is,

$$T^* = \frac{1}{2\pi} K_o\left(\sqrt{\frac{i\omega}{\kappa}} r\right) \tag{7}$$

where r is the distance from the source point (ξ, η) to the observation point (x, y) and K_o is the modified Bessel's function of the second kind of order zero. Equation (7) can be rewritten with the use of mathematical identities[19],

$$T^* = \frac{1}{2\pi}\left[ker_o\left(\sqrt{\frac{\omega}{\kappa}} r\right) + i kei_o\left(\sqrt{\frac{\omega}{\kappa}} r\right)\right] \tag{8}$$

where ker_o and kei_o are the Kelvin functions of order zero. Note that the derivative of the fundamental solution with respect to the outward normal n of the boundary Γ is,

$$\frac{dT^*}{dn} = \left(\sqrt{\frac{\omega}{\kappa}}\right)\left(\frac{d_r}{2\pi r}\right)[ker_o'(s) + i kei_o'(s)] \tag{9}$$

where d_r is the component of r in the normal direction, $s = \sqrt{(\omega/\kappa)} r$, and the prime represents d/ds.

The first term of (5) can be rewritten from $\int_\Omega T(\nabla^2 T^* - (i\omega/\kappa)T^*)\, d\Omega$ to $-\int_\Omega T\Delta(\xi, \eta)\, d\Omega$ using the sifting property of the delta function. This allows (5) to become,

$$T(\xi, \eta) + \int_\Gamma \frac{dT^*}{dn} T \, d\Gamma = \int_\Gamma \frac{dT}{dn} T^* \, d\Gamma \tag{10}$$

Equation (10) can be used to calculate the temperature, $T(\xi, \eta)$, at any point internal to the boundary once all of the boundary values have been determined.

In order to find the solution on the boundary, the unknown T's and dT/dn's, the above equation must be modified by taking the source point to the boundary, requiring that the integrals in (10) be interpreted in the Cauchy Principal Value sense. Equation (10) then becomes,

$$\left(\frac{1}{2}, 0\right) T(\xi, \eta) + \int_\Gamma \frac{dT^*}{dn} T \, d\Gamma = \int_\Gamma \frac{dT}{dn} T^* \, d\Gamma \tag{11}$$

where the first coefficient is separated into real and imaginary parts to emphasize that T is complex-valued. It is now possible to calculate the boundary conditions which were previously unknown by reducing (11) to an algebraic system of equations.

Up to this point, no mention has been made of the initial conditions for the boundary value problem. In the Laplace transform the initial conditions naturally appear as a result of the transform itself. This does not occur with the Fourier transform, but results for problems with non-zero initial conditions can still be obtained. First, let the temperature of the body be

represented by,

$$T(\bar{x}, t)=\bar{T}(\bar{x}, t)+T_{\infty}(\bar{x}) \tag{12}$$

where $\bar{x}$ is a position vector, t is time, $\bar{T}$ is the transient part of the solution, and T_{∞} is the initial condition. Substitution of this relation into (1) gives,

$$\nabla^2\bar{T}+\nabla^2T_{\infty}=\frac{1}{\kappa}\frac{\partial\bar{T}}{\partial t} \tag{13}$$

If $\nabla^2T_{\infty}=0$, which is common among engineering problems, then the transient problem is solved using (10) and (11) by substituting $\bar{T}$ for T in the derivation. The final solution, including any initial conditions, can then be found from (12). If T_{∞} does not satisfy Laplace's equation, then the contribution of the initial conditions to the problem must be determined using a domain integral. Problems of this nature are not efficiently solved using boundary elements since the main advantage of the method over finite elements, not discretizing the domain, is no longer valid.

Computer implementation

The integrals of (11) are approximated using numerical quadrature, dividing the boundary into N elements over which the temperature T and the heat flux $q=k(\mathrm{d}T/\mathrm{d}n)$ are taken as constant values. Equation (11) reduces to the following for the ith element on the boundary that is discretized into N elements,

$$k\left(\frac{1}{2}, 0\right)T^i+\sum_{j=1}^{N}T^j\int_{\Gamma_j}q^*\,\mathrm{d}\Gamma=\sum_{j=1}^{N}q^j\int_{\Gamma_j}T^*\,\mathrm{d}\Gamma \tag{14}$$

Writing these integrals in matrix form as,

$$\tilde{H}^{ij}=\int_{\Gamma_j}q^*\,\mathrm{d}\Gamma \tag{15a}$$

$$G^{ij}=\int_{\Gamma_j}T^*\,\mathrm{d}\Gamma \tag{15b}$$

and letting $H^{ij}=\tilde{H}^{ij}$ when $i\neq j$ and $H^{ij}=\tilde{H}^{ij}+k(\frac{1}{2}, 0)$ when $i=j$, (14) can be condensed into,

$$\boldsymbol{HT}=\boldsymbol{GQ} \tag{16}$$

where $\boldsymbol{H}$ and $\boldsymbol{G}$ are each complex $N\times N$ matrices, called the influence matrices of the system, and $\boldsymbol{T}$ and $\boldsymbol{Q}$ are complex-valued vectors of length N.

In general, the matrix entries in $\boldsymbol{G}$ and $\boldsymbol{H}$ are computed numerically in DYNBEMP using four-point Gaussian quadrature to perform the integration. For the case $i=j$, the integrals must be handled with care due to the singularity which occurs in the fundamental solution when the distance between the source and the observation points approaches zero. Here, the numerical integration is performed using a special Gaussian quadrature developed for logarithmic singularities[19].

Once the influence matrices have been determined, the boundary conditions for the particular problem are applied. Each element of the discretized boundary has a known value of temperature or heat flux acting upon it. As a result, unknown boundary values still remain on both the left and the right sides of (16). Collecting the unknowns on the left of the equation results in,

$$\boldsymbol{AX}=\boldsymbol{F} \tag{17}$$

where the vector $\boldsymbol{X}$ contains all the unknown boundary conditions.

The previous steps are followed for each significant frequency in the input spectrum (derived from an FFT of the time domain boundary conditions) and the entire solution stored. Then, an inverse FFT is applied to recover the time response at a given boundary location or point

interior to the body. Significant frequencies are determined from the FFT amplitude spectrum of the known boundary conditions by comparing the amplitude of a given frequency to the maximum amplitude contained in the FFT amplitude spectrum. If the ratio of the given frequency's amplitude to the maximum amplitude was less than 0.01, then that frequency was deemed insignificant, and the solution for that frequency is not included in the reconstruction, (2). Only frequencies less than the Nyquist frequency are operated on with this process. The Nyquist value is defined as $\omega_{Ny}=1/(2\Delta t)$, where Δt is the time step used in the FFT. Values above the Nyquist are not used in the DYNBEMP solution. This particular selection method was utilized for its ease of implementation and its accuracy. Since each frequency solution is calculated independently of the others, this process is a prime candidate for implementation on parallel processing machines.

The initial condition is taken to be zero for the BEM program, and any non-zero initial condition which satisfies Laplace's equation is accounted for, after the frequency solution has been found and inverted, using the procedure detailed in the previous section.

NUMERICAL EXAMPLES

Two-dimensional half space problem

To determine the applicability of the spectral boundary method to frequency domain results, a fully two-dimensional example is investigated. This problem consists of a semi-infinite half space with a heat flux, $\hat{Q}$, applied over the infinite strip $-a<x<a$, $y=0$, and $-\infty<z<\infty$. *Figure 2(a)* depicts this geometry.

The analytical frequency solution for this problem is obtained from the governing equation of heat conduction, as written in spectral form (2). Noting that $\hat{T}$ is an even function in x and can be written as a cosine series and then applying the following boundary conditions,

$$\hat{T}(y,\omega) \quad \text{and} \quad \frac{d\hat{T}}{dn} \quad \text{are finite as } y\to\infty$$

$$k\frac{d\hat{T}}{dn}=\hat{Q}_o \quad \text{at } y=0$$

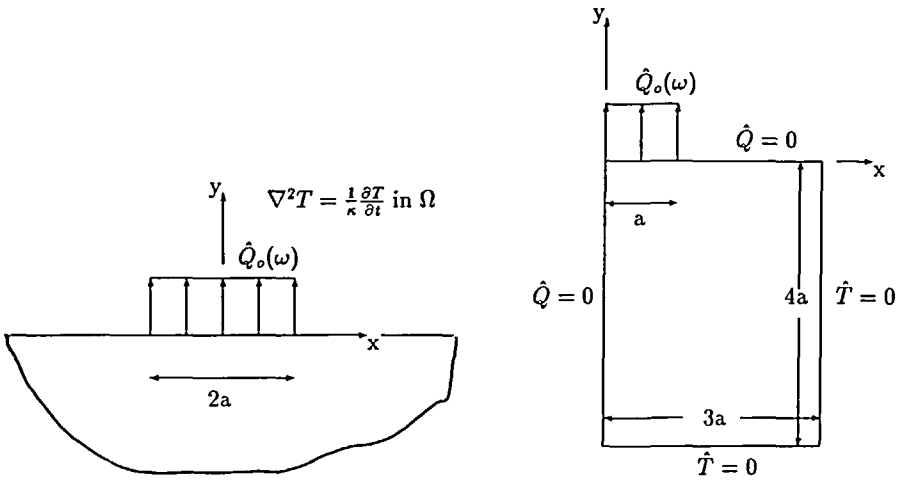

(a) Half space problem geometry (b) Boundary element model

Figure 2 (a) Actual geometry of the two-dimensional half-space example and (b) the DYNBEMP model

yields the complete frequency domain solution for this half space problem:

$$\hat{T}=\int_0^{\infty}\frac{-2\hat{Q}_o}{\pi k}\left[\frac{\sin\gamma a}{\gamma\sqrt{\gamma^2+\dfrac{i\omega}{\kappa}}}\right]\cos\gamma x\exp[-\sqrt{\gamma^2+(i\omega/\kappa)}y]\,d\gamma \tag{18}$$

This frequency domain solution may be interpreted in the time domain as the solution to the following steady-state problem: $Q_o(t)=\|\hat{Q}_o\|\sin(\omega t-\phi_Q)$ and $T(t)=\|\hat{T}\|\sin(\omega t-\phi_T)$, where $\|\hat{D}\|=\sqrt{(Re[\hat{D}])^2+(Im[\hat{D}])^2}$ is the amplitude and $\phi_D=\arctan(Im[\hat{D}]/Re[\hat{D}])$ is the phase. D represents either Q_o or T, the input heat flux and the temperature at a point in the half space, respectively.

In order to compare this analytical solution to results from DYNBEMP, the constants a, Q_o/k and κ were assigned values of 0.5 m, $1000+1000i$ °C/m and 1.48×10^{-5} m^2/s, respectively. The frequency, ω, used was 0.01 rad/s. The entire half space cannot be modelled with the constant element type utilized in DYNBEMP, so a block which is large enough to simulate a half space was used. The geometry of this block is shown in *Figure 2(b)*.

The DYNBEMP results are compared to the analytical solution along the surface ($y=0$, $0<x/a<1$) and along the centreline ($x=0$, $-1<y/a<0$). *Figures 3* and *4* depict the comparison for the real and imaginary parts of the complex temperature on the surface, and *Figures 5* and *6* contain the same results for the centreline temperature.

The maximum error encountered in this example is approximately 0.8% for either the real or imaginary parts of the complex temperature, excluding the few points near the centreline on the surface (*Figures 3* and *4*). The DYNBEMP results have a larger error on the surface near the centreline due to accuracy problems near sharp corners of a BEM model. This problem is discussed in detail in Reference [18]. The error encountered on the surface results in an error of phase and not in amplitude, as the real part of the temperature is overestimated and the imaginary part underestimated by approximately equal amounts.

Circular hole subjected to heat flux

Time domain reconstruction is examined using the example of an infinite body, with a hole of radius a in the centre, which has a known heat flux per unit length in the z-direction, $\bar{Q}$, applied to it. The problem geometry is depicted in *Figure 7*.

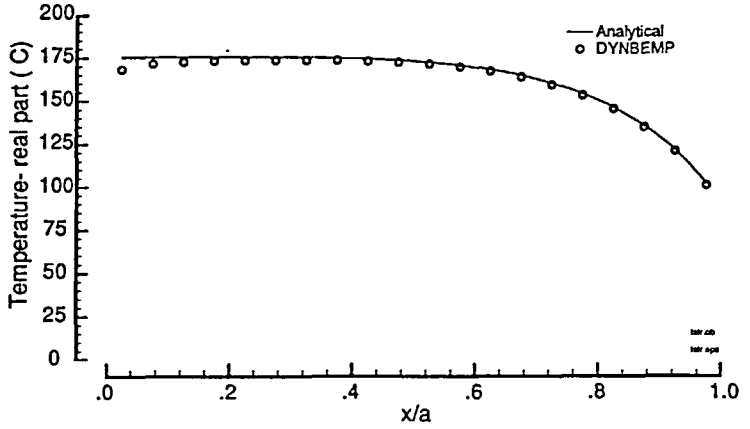

Figure 3 The real part of the complex temperature, for both the analytical and BEM solutions, determined along the surface of the half space ($y=0$) for frequency $\omega=0.001$ rad/s

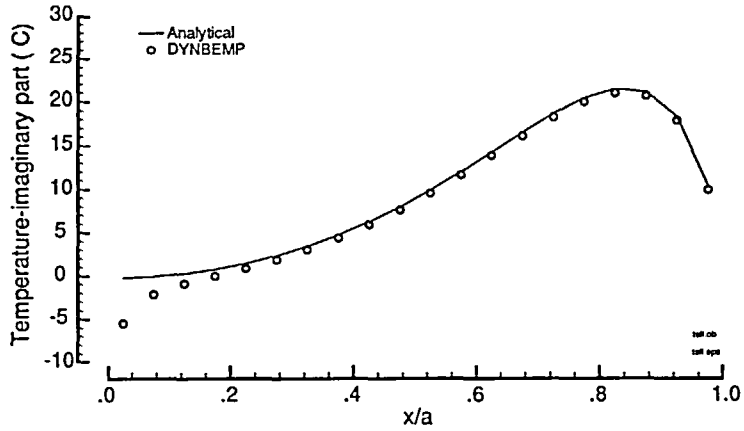

Figure 4 The imaginary part of the temperature, for both the analytical and BEM solutions, determined along the surface of the half space ($y=0$) for frequency $\omega=0.001$ rad/s

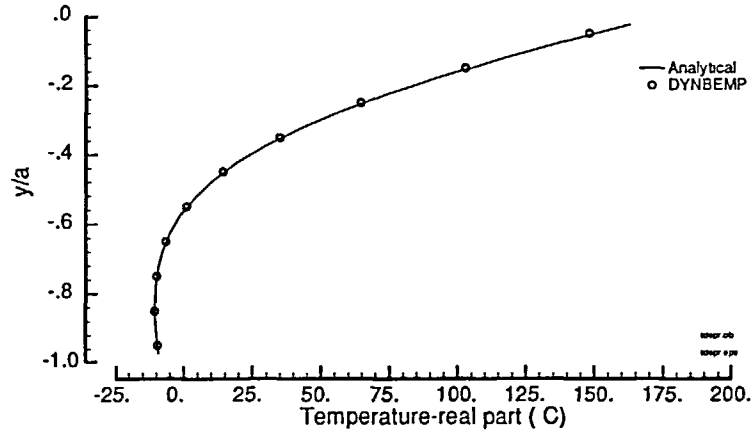

Figure 5 The real part of the temperature, for both the analytical and BEM solutions, determined along the centreline of the half space ($x=0$) for frequency $\omega=0.001$ rad/s

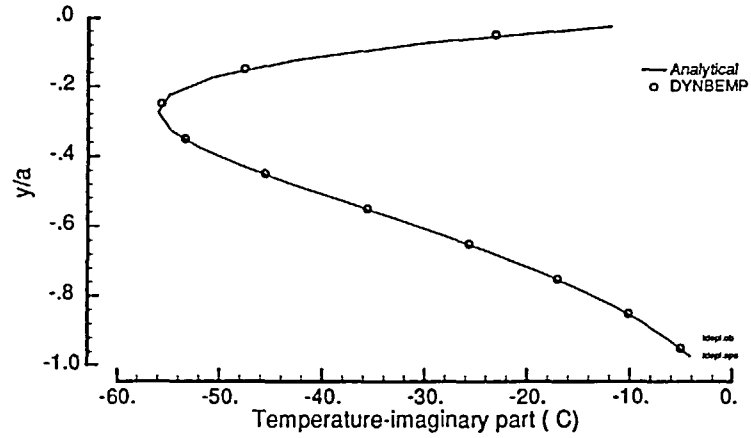

Figure 6 The imaginary part of the temperature, for both the analytical and BEM solutions, determined along the centreline of the half space ($x=0$) for frequency $\omega=0.001$ rad/s

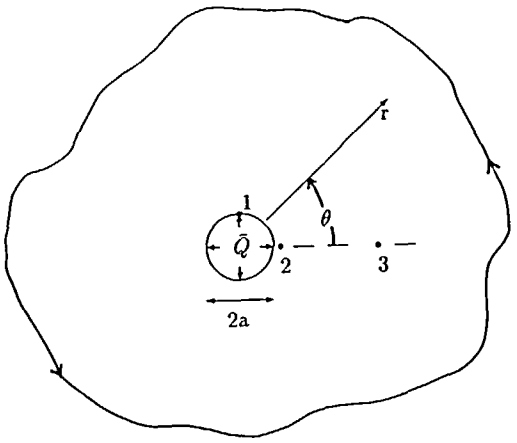

Figure 7 A hole in an infinite body with a surface flux applied to the hole boundary is the one-dimensional example. Locations for temperature reconstructions are indicated by points 1, 2 and 3 representing $r/a=1.0$, $r/a=1.1$ and $r/a=3.1$, respectively

The analytical solution for this problem can be obtained from the governing equation of heat conduction in spectral form as written in cylindrical coordinates, noting that the problem is symmetric with respect to θ:

$$\frac{\partial^2 \hat{T}_n}{\partial r^2}+\frac{1}{r}\frac{\partial \hat{T}_n}{\partial r}-\frac{i\omega_n}{\kappa}\hat{T}_n=0 \tag{19}$$

where $\hat{T}_n$ represents a complex-valued spectral temperature. Application of the following boundary conditions to the general solution of (19)[17],

$$\hat{T} \quad \text{and} \quad \frac{\mathrm{d}\hat{T}}{\mathrm{d}n} \quad \text{are finite as } r\to\infty$$

$$k\frac{\mathrm{d}\hat{T}}{\mathrm{d}n}=\bar{Q} \qquad \text{at } r=a$$

yields the complete frequency domain solution:

$$\hat{T}(r,\omega_n)=\frac{-\bar{Q}}{k\sqrt{\frac{\omega_n}{\kappa}}\left[ker_o'\left(\sqrt{\frac{\omega_n}{\kappa}}a\right)+ikei_o'\left(\sqrt{\frac{\omega_n}{\kappa}}a\right)\right]}\left[ker_o\left(\sqrt{\frac{\omega_n}{\kappa}}r\right)+ikei_o\left(\sqrt{\frac{\omega_n}{\kappa}}r\right)\right] \tag{20}$$

In order to compare this analytical solution to the results of DYNBEMP, the following numerical values were selected for the necessary constants: $\kappa=1.48\times10^{-5}$ m^2/s; $\omega_n=0.01$ rad/s; $a=0.5$ m; and $\bar{Q}/\kappa=1000+1000i\,°C/m$.

This problem was modelled with 20 constant boundary elements in DYNBEMP to approximate the hole boundary. These elements are suitable for two-dimensional problems and advantage is not taken of the axial symmetry. This is the only boundary which need be discretized. The elements are numbered clockwise, indicating that the normal to the boundary is directed inward, and the body itself lies outside the hole and extends to infinity. The temperatures obtained from the boundary element method are compared to the analytical values not only on the hole boundary, but also interior to the body (using (10)). In particular, the complex-valued frequency

domain temperatures $\hat{T}$ are determined along a radial line, for $1.0 < r/a < 5.1$ (see *Figure 7* for these locations). *Figures 8* and *9* depict these results for the real and imaginary parts of the complex temperature, respectively. These spectral boundary element results compare very well with the analytical solution, both for the temperature on the boundary (at $r/a = 1.0$) and points interior to the body (for $r/a > 1.0$). The maximum percent error encountered in this example was approximately 0.5% for either the real or imaginary part of the solution.

To solve this problem in the time domain requires a known flux history, which is applied to the hole boundary, from which the frequency spectrum can be obtained. The flux input selected is triangular in shape, with a width of 65 seconds and a peak magnitude $\bar{Q}/k = 1000\,^{\circ}\text{C/m}$. *Figure 10* shows this input flux history. The pulse has an initial time delay of ten seconds so that potential wrap-around problems in the FFT reconstructions are more readily apparent. For the FFT a time step of 0.5 seconds was used in combination with 1024 points to yield a total time window of 512 seconds, approximately seven times the duration of the input pulse. This should

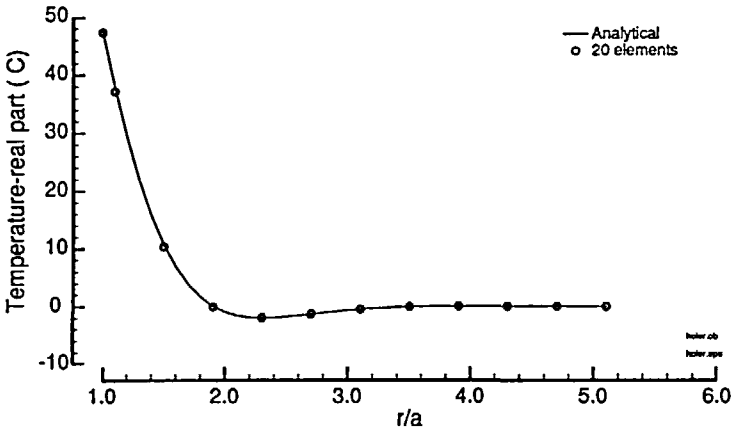

Figure 8 The real part of the complex temperatures, both analytical and BEM solutions, determined along a radial line for $\omega = 0.01$ rad/s

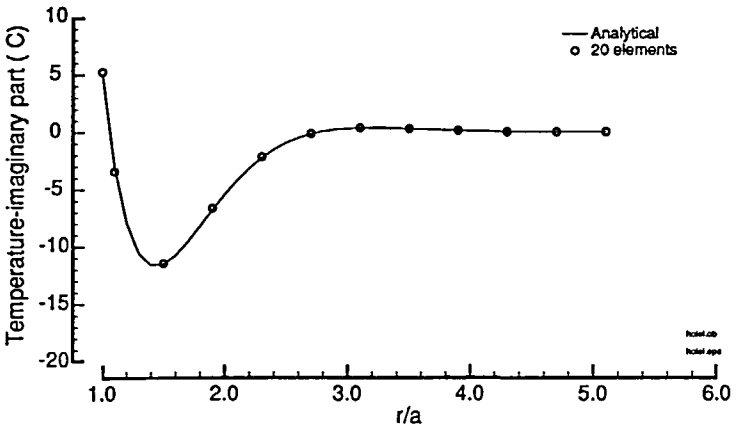

Figure 9 The imaginary part of the temperatures, both analytical and BEM solutions, determined along a radial line for $\omega = 0.01$ rad/s. The complete solution is the combination of both the real and imaginary parts of the frequency domain solution

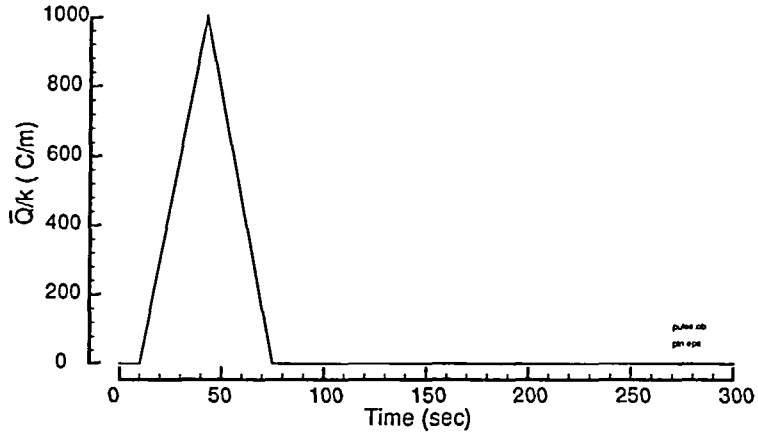

Figure 10 The time history of the applied flux on the hole boundary

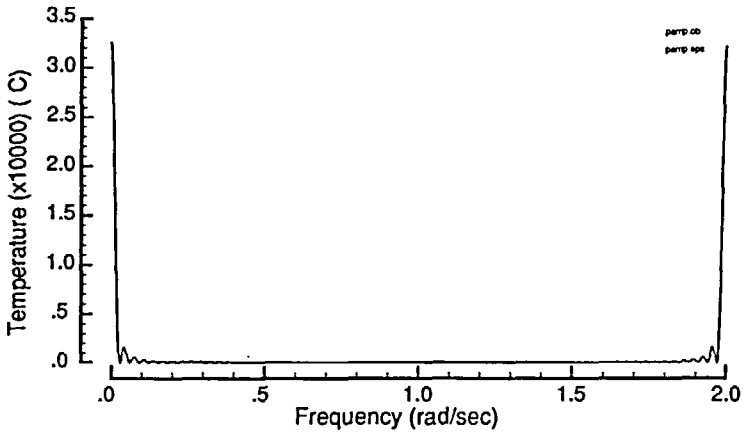

Figure 11 Amplitude spectrum of the applied flux resulting from the application of the FFT with the parameters $\Delta t = 0.5$ seconds and 1024 transform points

allow for the temperature at any point to return to zero before the end of the FFT window, eliminating any wrap-around problems. *Figure 11* represents the input pulse in the frequency domain after transformation with the above parameters. The FFT procedure used here is described in detail in Reference 15.

For the analytical transient solution, the frequency domain equation for the complex temperature (20) is solved for each and every frequency of the input spectrum (*Figure 11*) at a given location along a radial line. Then, the inverse FFT is implemented to transform this analytical frequency solution into the time domain.

To obtain DYNBEMP results, the frequency selection procedure was utilized, reducing the number of non-zero frequencies from 1023 to 34 (*Figure 11*). The entire solution for the boundary and the selected interior points is stored for each significant frequency so that time reconstructions of any element can be performed.

Temperature histories for three different locations are compared: one on the hole boundary at $r/a = 1.0$, one located at $r/a = 1.1$ and the last one at $r/a = 3.1$. *Figure 7* depicts the locations

graphically. The comparison of BEM results and the analytical solutions can be found in *Figure 12*. The DYNBEMP results agree very well with the known analytical solution. The maximum error encountered at the peak temperature is no greater than 0.8% for any of the three locations investigated. These comparisons also validate the frequency selection procedure, since the analytical solutions use all of the spectrum frequencies while the DYNBEMP results are reconstructed using only the significant ones.

Convection problem-circular cooling passage

This third example is presented to show the accuracy of the results for convective boundary conditions and non-zero initial conditions. The geometry of this problem is the same as for the circular hole in the finite half space discussed in Section 3.2 and pictured in *Figure 7*. The boundary and initial conditions for this problem can be expressed as

$$T \text{ and } \frac{dT}{dn} \text{ are finite as } r \to \infty$$

$$k\frac{dT}{dn} = -h_f(T - T_f) \quad \text{at } r = a$$

$$T(r, 0) = T_o$$

where T_o is a constant for this case. Letting $T(r, t) = \bar{T}(r, t) + T_o$, writing T and $\bar{T}$ in spectral form, and solving the frequency domain governing (19) for $\bar{T}$ results in the analytical frequency domain solution,

$$\hat{\bar{T}}(r, \omega_n) = \frac{-h_f \hat{T}_f \left[ker_o\left(\sqrt{\frac{\omega_n}{\kappa}} r\right) + i\, kei_o\left(\sqrt{\frac{\omega_n}{\kappa}} r\right)\right]}{k\left\{\sqrt{\frac{\omega_n}{\kappa}}\left[ker'_o\left(\sqrt{\frac{\omega_n}{\kappa}} a\right) + i\, kei'_o\left(\sqrt{\frac{\omega_n}{\kappa}} a\right)\right] - \frac{h_f}{k}\left[ker_o\left(\sqrt{\frac{\omega_n}{\kappa}} a\right) + i\, kei_o\left(\sqrt{\frac{\omega_n}{\kappa}} a\right)\right]\right\}} \tag{21}$$

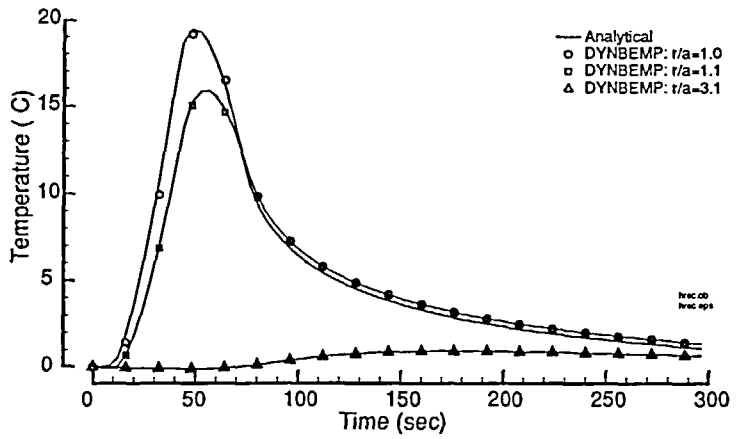

Figure 12 The temperature along the boundary of the hole, $r/a = 1.0$, and at two locations interior to the body $r/a = 1.1$ and $r/a = 3.1$, as determined from the analytical solution and the BEM

The complete solution in the time domain can be written as,

$$T(r, t) = T_o + \sum^{n} \hat{\hat{T}}(r, \omega_n)\, e^{i\omega_n t} \tag{22}$$

The numerical values of a and κ are the same as in the previous hole example, and T_o and h_f are assigned the values of 50°C and 1000 W/(m^2 – °C), respectively.

To simulate a pulse of cooling fluid through the hole, the time history selected for the known boundary condition T_f was initially at the body temperature $T_o = 50$°C (indicating an empty hole in thermal equilibrium with the body). Then the fluid begins flowing, dropping the temperature down 25°C and is maintained at this temperature for 60 seconds. The fluid flow is then stopped, and the temperature returned to the initial value (50°C). The initial time delay was again ten seconds to check for wrap-around in the FFT. DYNBEMP is used to solve for $\hat{\hat{T}}$ with T_o added after the inverse FFT has been performed. *Figure 13* represents the fluid (passage) temperature, with the initial condition value T_o retained. A time step of 0.1 seconds was used with 8192 points to yield a total time window of 819 seconds, more than ten times the input duration. *Figure 14* represents the frequency spectrum of the cooling liquid pulse after transform.

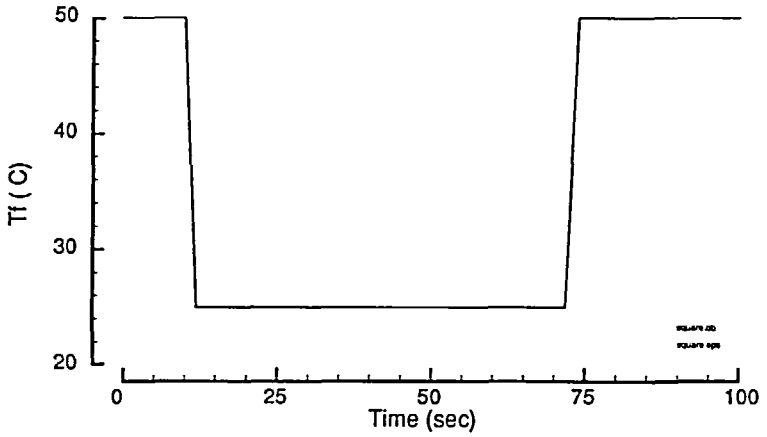

Figure 13 The temperature history of the cooling fluid in the circular hole

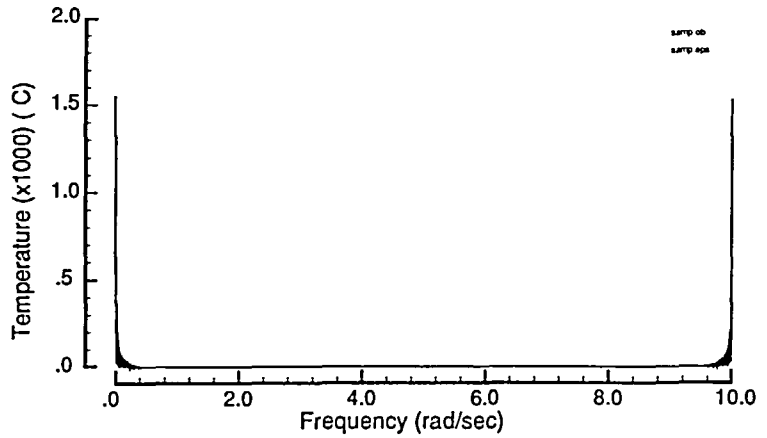

Figure 14 The FFT of the fluid temperature, after subtracting the initial conditions, using $\Delta t = 1$ second and $N = 8192$

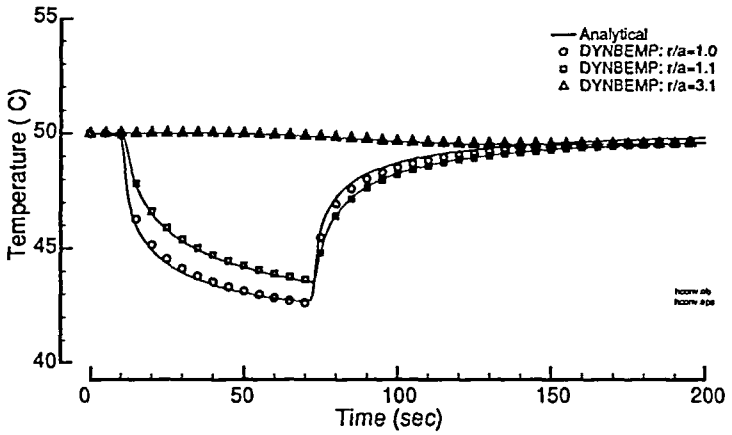

Figure 15 The temperature along the boundary of the hole, $r/a=1.0$, and at two locations interior to the body, $r/a=1.1$ and $r/a=3.1$, as determined from the analytical solution and the BEM. Initial condition has been added

The analytical solution is found using all of the frequencies and complex temperature values from the transform, while the frequency selection procedure discussed in the last example is performed on the input spectrum to reduce the number of non-zero frequencies from 8191 to 173. DYNBEMP only provides a solution for those 173 values. All other values have a zero solution.

Temperature histories for three different locations are compared: one on the hole boundary at $r/a=1.0$, one located at $r/a=1.1$ and one at $r/a=3.1$. *Figure 7* depicts these locations, which are the same as in the previous example. The comparison of the BEM results and the analytical solution in the time domain (after the initial conditions have been added) can be found in *Figure 15*. The DYNBEMP reconstructions are in error of no more than 0.7% for any of the three locations of interest. Again, the frequency selection procedure holds for the different input pulse and transform.

CONCLUSIONS

The spectral boundary element method, in conjunction with spectral analysis and the fast Fourier transform, is shown to be a useful tool for solving transient heat conduction problems. Both the half space and axisymmetric example problems validate the application of the spectral boundary element method to heat conduction problems. When compared to analytical solutions, the BEM produced very good agreement of results for all problems investigated, in both the frequency and time domains, and for both interior and boundary points. The fast Fourier transform procedure can be made very efficient by excluding frequencies whose FFT spectrum amplitides are small and do not substantially contribute to the overall problem solutions. Finally, it is noted that the FFT approach is uniquely suitable for massively parallel computation, as each processor could be used for a different frequency of the transform spectrum.

ACKNOWLEDGEMENT

The research was supported in part by the National Science Foundation under grant CDR 880317 to the Engineering Research Center for Intelligent Manufacturing Systems.

REFERENCES

1 Brebbia, C. A. and Dominguez, J. *Boundary Elements An Introductory Course*, Computational Mechanics Publications, Southampton, first edition (1988)
2 Becker, A. A. *The Boundary Element Method in Engineering: A complete course*, McGraw-Hill, New York (1992)
3 Banerjee, P. K. and Butterfield, R. *Boundary Element Methods in Engineering Science*, McGraw-Hill, London (1981)
4 Manolis, G. D. A comparative study on three boundary element method approaches to problems in elastodynamics, *Int. J. Num. Meth. in Eng.*, **19**, 73–91 (1983)
5 Beskos, D. E. Boundary element methods in dynamic analysis, *Appl. Mech. Rev.*, **40**(1), 1–23 (1987)
6 Israil, A. S. M. and Banerjee, P. K. Advanced development of time domain BEM for two-dimensional scalar wave propagation, *Int. J. Num. Meth. in Eng.*, **29**, 1003–1020 (1990)
7 Liggett, J. A. and Liu, P. L.-F. Unsteady flow in confined aquifers: a comparison of two boundary integral methods, *Water Resources Res.*, **15**, 861–866 (1979)
8 Cheng, A. H.-D. and Ou, K. An efficient Laplace transform solution for multiaquifer systems, *Water Resources Res.*, **25**, 742–748 (1989)
9 Vardoulakis, I. and Harnpattanapich, T. Numerical Laplace-Fourier transform inversion technique for layered soil consolidation problems. *Int. J. Num. and Anal. Meth. in Geomechanics*, **10**, 347–365 (1986)
10 Rizzo, F. J. and Shippy, D. J. A method of solution for certain problems of transient heat conduction, *AIAA J.*, **8**, 2004–2009 (1970)
11 Ding, J. Application of the BEM to unsteady heat transfer problems, *J. of Aerospace Power*, **19**, 110–114 (1989)
12 Moridis, G. J. and Reddell, D. L. The Laplace Transform Boundary Element (LTBE) numerical method for the solution of diffusion-type equations, *Boundary Elements XIII*. Computational Mechanics Publications, Southampton and Elsevier, London (1991)
13 Lachat, J. C. and Combescure, A. Laplace transform and boundary integral equation: application to transient heat conduction problems, *Proc. First Symp. on Innovative Num. Anal. in Applied Eng. Science*, CETIM (1977)
14 Lafe, O. Fourier transform and boundary element simulation of 3-D flow in a leaky porous medium, *Proc. of BETECH V*, Computational Mechanics Publications (1990)
15 Doyle, J. F. *Wave Propagation in Structures: An FFT-based spectral analysis methodology*, Springer-Verlag New York, Inc., New York, first edition (1989)
16 Yang, Shi Chao and Zheng, G. R. Boundary element method applied to steady periodic heat conduction, *Num. Heat Transfer*, **19**, 117–124 (1991)
17 Carslaw, H. S. and Jaeger, J. C. *Conduction of Heat in Solids*, Oxford University Press, Glasgow, second edition (1959)
18 Hucker, S. A. and Farris, T. N. Modified crack closure method using boundary elements, *Eng. Fracture Mech.*, **46**(5), 763–772 (1993)
19 Abramowitz, M. and Stegun, I. *Handbook of Mathematical Functions with formulas, graphs, and mathematical tables*, chapter 9, 25, Dover Publications, New York (1972)